MODELING CATHODE ROUGHNESS, WORK FUNCTION, AND FIELD ENHANCEMENT EFFECTS ON ELECTRON EMISSION*

D. A. Dimitrov, G. I. Bell, D. Smithe, S. Veitzer, Tech-X Corp., Boulder, CO 80303, USA
I. Ben-Zvi, J. Smedley, BNL, Upton, NY 11973, USA
J. Feng, S. Karkare, H. A. Padmore, LBNL, Berkeley, CA 94720, USA

Abstract

Recent developments in material design and growth have resulted in photocathodes that can deliver high quantum efficiency and are sufficiently robust to use in high electric field gradient photoinjectors and free electron lasers. The growth process usually produces photoemissive material layers with rough surface profiles that lead to transverse accelerating fields and possible work function variation resulting in emittance growth. To better understand the effects of surface roughness on emitted electron beams, we have developed realistic three-dimensional models for photocathode materials with grated surface structures. They include general modeling of electron excitation due to photon absorption, charge transport and emission from rough surfaces taking into account image charge and field enhancement effects. We implemented these models in the VSim particle-in-cell code. We report results from simulations using different photocathode materials with grated and flat surfaces to investigate how controlled roughness, work function variation, and field enhancement affect emission properties.

INTRODUCTION

Effective operation of free electron lasers (FELs), linear accelerator facilities and advanced X-ray light sources, depends on providing reliable photocathodes [1] for generation of low emittance, high-brightness, high-current electron beams using conventional lasers. Modern developments in design and synthesis of materials have resulted in photocathodes that can have a high quantum efficiency, operate at visible wavelengths, and are robust enough to operate in high electric field gradient photoguns, for application to FELs, in dynamic electron microscopy and diffraction. Synthesis, however, often results in roughness, ranging from the nano to the microscale. Thus, the effects on roughness on emittance are of significant importance to understand.

Recently, advances in material science methods have been demonstrated to control the growth of photoemissive materials, e.g. Sb on a Si substrate, to create different types of rough layers with a variable thickness of the order of 10 nm. A new momentatron experiment concept was developed [2] to measure transverse electron momentum and emittance. A successful application of the momentatron concept was demonstrated by Feng *et al.* [3] to investigate the thermal limit of intrinsic emittance from flat surfaces. Their experiments provide reference data on intrinsic emittance from

Sb cathodes. The effects of surface roughness can then be evaluated relative to the flat emission surface measurements.

Although analytical formulations of the effects of roughness have been developed, a full theoretical model and experimental verification are lacking. Our work aims to bridge this gap. We report results on electron emission modeling and 3D simulations from photocathodes with controlled surface roughness similar to grated surfaces that have been fabricated by nanolithography.

MODELING

We use the VSim Particle-in-Cell (PIC) code to to simulate electron emission from photocathodes with flat and controlled rough surfaces. Our approach includes electron excitation in response to absorption of photons with a given wavelength, charge dynamics due to drift and various types of scattering processes, representation of flat and rough interfaces, calculation of electron emission probabilities that takes into account image charge and field enhancement effects across rough surfaces, particle reflection and emission updates, and efficient 3D electrostatic (ES) solver for a simulation domain that has sub-domains with different dielectric properties.

Electron excitation is modeled with exponential decay of absorbed laser light intensity relative to positions on the photocathode surface. Electrons can be excited due to normal or oblique light incidence (relative to a reference plane). In Sb, electrons are selected for excitation from occupied states at a given temperature T in the conduction band from the distribution $p(E) = g(E)f_{FD}(E)$, where $g(E)$ is the density of states (DOS) obtained from Bullett [4] and $f_{FD}(E)$ is the Fermi-Dirac function. Electrons are created only if their final state with energy $E + \hbar\omega$ is not occupied (with probability $1 - f_{FD}(E + \hbar\omega)$) where $\hbar\omega$ is the photon energy.

In VSim, charge transport is modeled based on the ensemble Monte Carlo method. We have implemented it for two semiconductors: diamond [5] and GaAs [6]. These models take into account different types of electron and hole scattering processes. For metallic materials, electron-electron (el-el) scattering is the dominant process that affects emission. Often, a single el-el scattering event will reduce the energy of an excited electron below its threshold for emission. We have implemented a unified model for el-el scattering in metals proposed by Ziaja *et al.* [7]. It is applicable over a wide range of energies and is efficient for use in Monte Carlo transport simulations. The electron mean free path

(MFP), $\lambda(E)$, is given by the simple formula:

$$\lambda(E) = \frac{\sqrt{E}}{a\,(E - E_{th})^b} + \frac{E - E_0 \exp(-B/A)}{A \ln(E/E_0) + B}, \quad (1)$$

where the initial electron impact energy E is in eV, E_{th} is the effective energy threshold for production of an electron-hole pair as a result of the scattering, $E_0 = 1$ eV, and a, b, A, and B are fitting parameters with units that give the MFP in Å. For metals, $E_{th} = E_F$, where E_F is the Fermi energy ($E_{th} = E_G$ in semiconductors with E_G the energy gap). The fitting parameters are determined using experimental data and/or full band structure calculations. The parameters a and b determine the MFP at the low energy regime ($E_{F/G} < E < E_P$, where E_P is the plasmon energy). This is the regime of interest to electron emission from metallic materials. In this regime and assuming the speed of electrons is given by $v(E) = \sqrt{2E/m^*}$, where m^* is the electron effective mass, the el-el scattering rate is given by $\Gamma(E) \approx \tilde{a}\,(E - E_{th})^{d+0.5}$, where $\tilde{a} \equiv a\sqrt{2/m^*}$ and $d \equiv b - 0.5$. The free electron gas model and Fermi-liquid theory both lead to $b = 2$ while Ziaja et al. [7] have used Eq. (1) to fit experimental data for a number of metals to obtain values for the model parameters. Their data showed values in the range $1.5 \le b \le 5.0$ or $1.0 \le d \le 4.5$.

Since we currently do not have data for el-el scattering in Sb, we bracketed the rates using a lower and a higher rate, shown in Fig. 1, selecting d from the range of values reported for a number of other metals [7]. When an electron
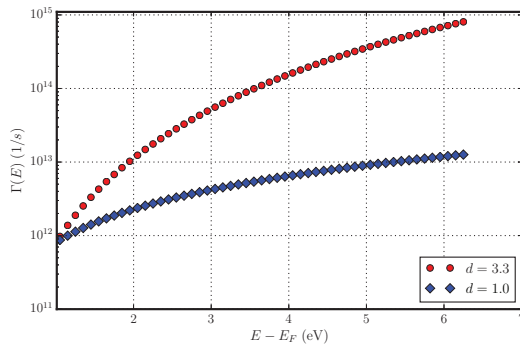

Figure 1: The shown el-el scattering rates were used in the runs for modeling Sb photocathodes.

from inside the photocathode attempts to cross the emission surface, a probability of emission is calculated using our implementation of the transfer matrix (TM) method [8] with a surface potential determined at the location of the crossing and along the outward normal. This allows us to take into account the field enhancement effect.

RESULTS

We ran simulations with the implemented models to investigate how surface roughness and two different el-el scattering rates affect the spectral response of quantum yield and intrinsic emittance. For modeling emission from flat and three-ridge rough Sb surfaces, we ran most of the simulations with a uniform work function of $\phi = 4.5$ eV and used

periodic boundary conditions along the transverse directions (y and z). There is a constant potential difference maintained across the x length of the simulation domain leading to an applied field magnitude in the vacuum region of the order of 1 MV/m. The field varies on the rough emission surface.

The intrinsic emittance, per mm of rms laser spot size, is given by $\epsilon_y/\sigma_y = \sqrt{\langle p_y^2 \rangle}/m_e c$, where σ_y is the laser spot size in mm, m_e is the electron mass in vacuum, c is the speed of light, and p_y is one of the transverse momentum components of electrons at emission. A theory [3] (and references therein) based on several approximations gives:

$$\langle p_y^2 \rangle / m_e = (\hbar\omega - \phi)/3. \quad (2)$$

A more accurate treatment of DOS and temperature effects [3] leads to:

$$\frac{\langle p_y^2 \rangle}{m_e} = \frac{\displaystyle\int_{E_F+\phi-\hbar\omega}^{\infty} dE\, p(E)(E + \hbar\omega) h(E, \phi, \hbar\omega)}{\displaystyle\int_{E_F+\phi-\hbar\omega}^{\infty} dE\, p(E)(E + \hbar\omega)\left(1 - \sqrt{\frac{E_F+\phi}{E+\hbar\omega}}\right)}, \quad (3)$$

where $h(E, \phi, \hbar\omega) = \frac{2}{3} - \sqrt{\frac{E_F+\phi}{E+\hbar\omega}} + \frac{1}{3}\left(\frac{E_F+\phi}{E+\hbar\omega}\right)^{\frac{2}{3}}$. In the simulations, we can calculate the mean transverse energy (MTE) of emitted electrons at emission and when they cross a diagnostic surface in a given location in vacuum. The MTE is then used to obtain the intrinsic emittance and compare with the models given by Eq. (2) and Eq. (3).
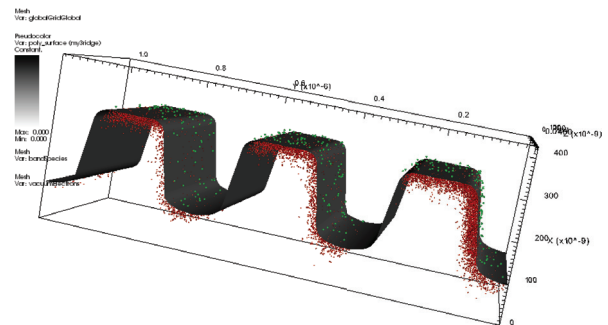

Figure 2: Electrons are loaded in Sb only at $t = 0$ s (red spheres; light impacts at an angle) and within a layer of 20 nm from the rough interface (the gray surface). Electrons emitted in vacuum are shown with green spheres.

The controlled rough surface has a ridge period of 394 nm, ridge height of 194 nm, and a width of the ridge flat top of 79 nm. The three ridge rough surface is shown in Fig. 2 together with excited electrons and their distribution at a given time. The simulation domain size for both the 3-ridge and the flat emission surfaces is $0.4268 \times 1.182 \times 0.394$ all in μm along x, y, and z respectively with $88 \times 264 \times 16$ number of cells. We implemented an efficient algorithm that loads a specific number of electrons above a given energy threshold (while recording how many electrons were excited to reach this goal). This is needed to calculate quantum yield (QY) and to make it possible to explore the emission regime

05 Beam Dynamics and Electromagnetic Fields

D11 Code Developments and Simulation Techniques

when the photon energy decreases below the work function. The algorithm also removes electrons in the photocathode if
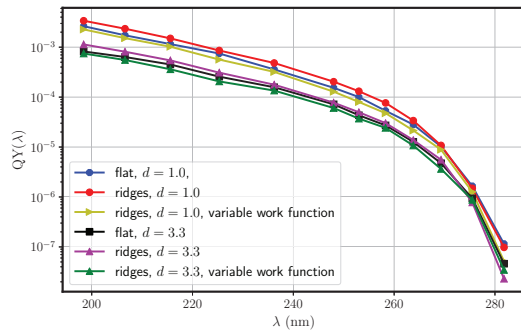

Figure 3: Simulation results on QY for emission from flat and rough Sb surfaces.

their energy falls below a given threshold value. In metals, one el-el scattering event usually reduces the energy of an excited electron enough to make it ineligible for emission. All runs started with 3×10^5 excited electrons with energies $E > E_F + 4.4$ eV. For the highest photon energy $\hbar\omega = 6.25$ eV, this goal was reached after exciting 7.8×10^5 electrons, while for the lowest one $\hbar\omega = 4.4$ eV, around 1.7×10^8 electrons had to be excited. The absorption length in Sb is ≈ 10 nm over this interval of photon energies.

The results shown in Fig. 3, indicate that using a uniform work function leads to higher QY for emission from the rough surface compared to the flat one. This is likely due to a geometric effect: for normal light incidence, electrons absorbed on the sides of the ridges are closer to the emission surface than in the case of the flat surface. Using a variable work function (higher on the sides of the ridges) lowers the QY below the values from the flat emission surface. As expected, increasing the el-el scattering rate, decreases the QY (the effective electron lifetime for emission decreases).
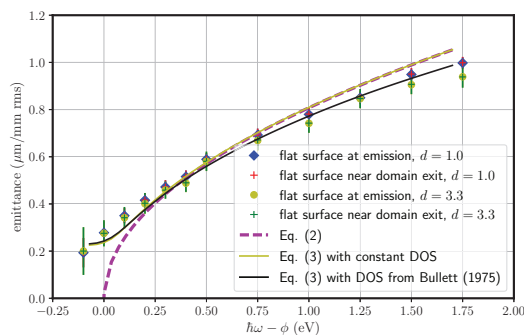

Figure 4: For Sb with a flat surface, the intrinsic emittance from the simulations is in good agreement with theory and experimental data [3].

Results on intrinsic emittance from simulations with a flat Sb surface, shown in Fig. 4, are in good agreement with the theory given by Eq. (3). This level of agreement is only possible if both the finite temperature and accurate DOS effects are included in the modeling. For the flat surface, the transverse electric fields in vacuum is practically zero. Thus, the MTE does not change. This is confirmed by the data in

Fig. 4: the intrinsic emittance at emission and at a diagnostic surface near the exit of the simulation is approximately the same.

Results on intrinsic emittance from the controlled rough surface are shown in Fig. 5. As expected, the intrinsic emittance increases compared to the results from the flat Sb surface. This is due to emission from the sides of the ridges and the presence of transverse electric fields between them. Due to field enhancement and the Schottky effect, the largest probability of emission is near the edges of the ridges.
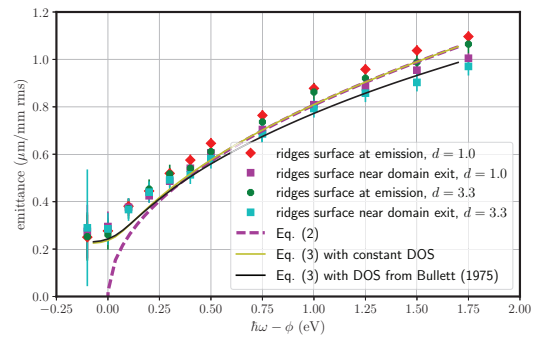

Figure 5: Intrinsic emittance for emission from the rough Sb surface is higher compared to the flat one. Decreasing the el-el scattering rate increases the intrinsic emittance.

SUMMARY

We implemented models to simulate electron emission from Sb photocathodes with controlled rough surfaces in the 3D VSim PIC code. The implementation includes accurate and efficient treatment of DOS and Fermi-Dirac distribution effects in both the excitation of electrons due to photon absorption and in handling el-el scattering. This allows modeling of emission even when the photon energy decreases below the work function and only electrons excited from the tail of the Fermi-Dirac distribution (with energies $E > E_F$) could be emitted. Simulation results on emission from flat Sb surfaces show spectral response of the intrinsic emittance that is good agreement with theory and experimental data [3]. Emission from rough surfaces leads to increase of the intrinsic emittance. Simulation results with the higher el-el scattering rate are in better agreement with the theory and data on intrinsic emittance from flat Sb surfaces.

REFERENCES

[1] D. H. Dowell *et al.*, *Nucl. Instr. Meth. Phys. Res. A*, vol. 622, p. 685, 2010.

[2] J. Feng *et al.*, *Rev. Sc. Instr.*, vol. 86, p. 015103, 2015.

[3] J. Feng *et al.*, *Appl. Phys. Lett.*, vol. 107, p. 134101, 2015.

[4] D. W. Bullett, *Solid State Commun.*, vol. 17, p. 965, 1975.

[5] D. A. Dimitrov *et al.*, *J. Appl. Phys.*, vol. 108, p. 073712, 2010.

[6] S. Karkare *et al.*, *J. Appl. Phys.*, vol. 113, p. 104904, 2013.

[7] B. Ziaja *et al.*, *J. Appl. Phys.*, vol. 99, p. 033514, 2006.

[8] D. A. Dimitrov *et al.*, *J. Appl. Phys.*, vol. 117, p. 055708, 2015.